Frontiers in Bioscience Elite

Front. Biosci. (Elite Ed) **2026**; 18(2): 47018
https://doi.org/10.31083/FBE47018

Original Research

Optimization and Characterization of Dried Distiller Grains With Solubles as a Sustainable Protein Isolate

Muhammad Haris[1], Ademola Hammed[1,2,*]

[1]Department of Agricultural and Biosystems Engineering, North Dakota State University, Fargo, ND 58102, USA
[2]Department of Environmental and Conservation Sciences, North Dakota State University, Fargo, ND 58102, USA
*Correspondence: Ademola.hammed@ndsu.edu (Ademola Hammed)
Academic Editor: Bikram Basak
Submitted: 29 September 2025 Revised: 9 December 2025 Accepted: 18 December 2025 Published: 15 June 2026

Abstract

Background: The increasing demand for sustainable and high-quality protein sources has driven research into the efficient extraction and characterization of proteins from various plants and industrial by-products. Dried distillers grains with solubles (DDGS) is a rich source of protein with potential applications in food and animal feed; however, the structural and nutritional properties of DDGS require further elucidation compared with those of soy protein isolate (SPI). **Methods**: Thus, this study aimed to optimize protein extraction from DDGS using response surface methodology, yielding a protein yield of approximately 23%. The extracted proteins were characterized by proximate analysis, sodium dodecyl sulfate–polyacrylamide gel electrophoresis (SDS-PAGE) to assess structural integrity, thermogravimetric analysis, differential scanning calorimetry, Fourier-transform infrared spectroscopy, and amino acid profiling. Comparative analyses with SPI were conducted to evaluate their structural, thermal, and nutritional differences. **Results**: The optimized extraction conditions included a 2-hour extraction time, a solid-to-liquid ratio of 1:10, 1 M sodium hydroxide (NaOH), and 60% ethanol. The crude protein content increased significantly from 24.94% in raw DDGS to 65.21% in the isolate. SDS-PAGE revealed intact globular protein bands in SPI, whereas DDGS proteins showed fragmentation, likely due to denaturation and interactions with fiber. Thermal analysis indicated that DDGS proteins possessed higher heat resistance and thermal stability than SPI. Amino acid analysis demonstrated the superior essential amino acid profile of SPI, which was rich in leucine, lysine, phenylalanine, and etc. In contrast, DDGS proteins contained valuable amino acids, including glutamic acid, aspartic acid, and branched-chain amino acids, making the DDGS proteins suitable for ruminant diets. These structural and compositional differences reflect the respective suitability of these sources for food versus feed applications. **Conclusions**: This study highlights the effectiveness of optimized extraction techniques for isolating high-protein concentrates from DDGS and emphasizes the distinct characteristics of DDGS proteins compared with SPI. While SPI remains ideal for nutritional formulations requiring high purity and amino acid completeness, DDGS proteins offer a sustainable alternative for livestock nutrition, especially in ruminant diets. These findings support the broader utilization of DDGS as an economical and environmentally sustainable protein source.

Keywords: DDGS; SPI; protein extraction; hydrolysis; characterization

1. Introduction

Distillers' dried grains with solubles (DDGS) serve as a widely utilized feed ingredient in the animal feed industry, valued for their high nutritional content and low production cost. DDGS are a by-product of the dry milling process, consisting of the undigested grain components remaining after the fermentation of grains during ethanol production [1]. In 2019, the United States produced approximately 22.6 million tons of DDGS. With the rising global demand for bioethanol as a transportation fuel, DDGS production is anticipated to continue increasing to meet both domestic and international market demands [2,3].

With the annual production of DDGS steadily increasing, there is growing interest in exploring and enhancing its applications. As a protein-rich material, containing approximately 30–40% protein on average, DDGS represents a promising resource for various bio-industrial applications, including the production of adhesives and resins [2,4]. However, these approaches often fail to capitalize on the high market value of extracted proteins and may compete with low-cost alternatives, such as the combustion of corn stover. An alternative and more economically viable strategy involves the separation and extraction of proteins from DDGS [5].

Protein extraction from DDGS presents significant challenges. Previous studies demonstrated that only 25% of protein could be extracted using sodium hydroxide [6]. The alkaline extraction method is still the most widely used technique for removing protein from maize-based DDGS, even though other approaches have been studied. Factors such as alkali concentration, extraction time, solid loading and temperature are critical determinants of extraction efficiency, with both independent and interactive effects that need to be optimized [7]. Previous studies have shown that there is need to quantify the optimization conditions using combination of Sodium Hydroxide (NaOH) and Ethanol as a dependent variable in the extraction of protein.

To address the complexity of optimizing these variables, response surface methodology (RSM) offers an effective solution. RSM is a statistical and mathematical framework designed for constructing empirical models and optimizing multivariate processes. It has been successfully applied in the optimization of chemical and enzymatic reactions [8].

The yields of active compounds and biomolecules from bioresources during the extraction process are controlled or determined by the process conditions (extraction time, temperature, particles sizes, solid loading and extraction agents) [7–9]. Similarly, to other rich industrial bioresources, DDGS has high value protein that could be extracted. Although extraction step increases processing cost, an efficient approach needs to be developed. This is achievable by investigating different extraction conditions to determine the optimum conditions. Therefore, we have set up experimental design that involves varying solid to liquid ratio, time, ethanol and NaOH concentration to optimize the extraction of protein from DDGS employing RSM to maximize extractability.

2. Methodology

2.1 Raw Material and Chemicals

In this experiment, the Blue Flint Ethanol Plant (Underwood, ND, USA) provided the DDGS sample. In preparation for the experiment, the material was kept between 4–6 °C. Throughout the investigation, the same batch of DDGS was utilized to minimize the variability in DDGS composition. Ethyl Alcohol 200 proof Anhydrous was purchased from ACROS. NaOH was purchased from EMD in pellets form which was later converted to the required concentrations.

2.2 Sample Preparation

Raw DDGS samples were ground in the Blendtec Designer 650 (Orem, UT, USA) to reduce the particle size. The ground samples were then subjected to the sieve analysis process; the sample size of 0.85–0.425 mm (preliminary study) was selected for the rest of the experiment. For the hydrolysis process, the temperature of the water bath was kept at 55 °C as a standard for all the experimental runs.

2.3 Experimental Design

RSM and central composite design (CCD) were used to examine how the four independent variables affected protein content and protein yield shown in Table 1. Thirty-one trial runs were conducted to optimize the extraction parameters. For every independent variable, there were five levels (–2, –1, 0, +1, +2). The protein yield (Y1) and protein concentration (Y2) are dependent variables, whereas the four independent variables are Ethanol (X1), NaOH concentration (X2), solvent ratio (X3), and extraction time (X4).

Table 1. Independent variables and their levels in CCD.

Variables	Levels					
	Codes	–2	–1	0	+1	+2
Ethanol (%)	X1	30	45	60	75	90
NaOH concentration (M)	X2	0.05	0.05	0.5	1	1
Solid to liquid ratio (w/v)	X3	1:5	1:5	1:10	1:15	1:15
Extraction Time (h)	X4	0.5	1	1.5	2	2

CCD, central composite design; NaOH, Sodium Hydroxide.

2.3.1 Protein Extraction

A central composite design was employed comprising 31 experimental runs, with independent variables including NaOH concentration (0.05, 0.5, and 1 M), ethanol concentration (30, 45, 60, 75, and 90%), sample-to-solvent ratios (1:5, 1:10, and 1:15), and extraction time (0.5, 1, 1.5, and 2 h). Samples were weighed according to the designated sample-to-solvent ratios (ranges between 2.5–7.5 g) and placed into 100 mL Erlenmeyer flasks. Subsequently, 50 mL of the solvent mixture was added to each flask, and the flasks were incubated at 55 °C while shaking at 200 rpm. Extractions were conducted in accordance with the time specified for each experimental run. The resulting extracts were centrifuged at 3000 rpm for 20 min to separate particulate and soluble fractions by decantation. The pH of the supernatants was adjusted to the protein isoelectric point (pH 5.5–6) using dilute HCl, and the solutions were allowed to precipitate overnight. The precipitated solutions were centrifuged again at 3000 rpm for 20 min. Following the second centrifugation, the supernatant was discarded, and the precipitate was washed with distilled water and oven-dried at 130 °C for 6 h using a Binder ED 56 ED056UL-120V Oven Dryer (BINDER GmbH, Tuttlingen, Baden-Württemberg, Germany).

2.3.2 Protein Quantification Using Bradford Method

Protein content in the extracts was determined using the Bradford assay. Bovine serum albumin (BSA) was employed to generate the protein standard curve [10]. Absorbance measurements were recorded at 595 nm using a TTecan Infinite 200 PRO (Tecan Group Ltd., Männedorf, Zurich, Switzerland).

2.4 Proximate Analyses

2.4.1 Moisture Content

Moisture content was determined following the AOAC 925.10 standard method [11]. Approximately 1 g of sample was weighed into a pre-weighed crucible and oven-dried at 105 °C for 24 h. The crucible weight was recorded prior to sample addition. Moisture content (%) was then calculated using Eqns. 1 & 1.1.

$$\% \text{ Mc } = \frac{\text{M}_w}{\text{S}_w} \times 1 \quad (1)$$

$$M_w = S_w - (D_c - E_c) \quad (1.1)$$

Mw = moisture weight, Sw = sample weight, Ec = empty crucible, and Dc = dried sample and crucible weight.

2.4.2 Ash Content

Total ash content was determined by incineration using a Thermo Fisher Scientific Thermolyne Benchtop TM 1100 °C muffle furnace (Vernon Hills, IL, USA). Approximately 2 g of each sample was weighed into a crucible and subjected to ashing at 575 °C for 24 h [12]. Following incineration, the crucibles were cooled in a desiccator, and the ash content was quantified according to Eqn. 2.

$$\% \text{ ash } = \frac{M2 - M1}{Ms} \times 100 \quad (2)$$

M2 = Weight of ash. M1 = Weight of crucible. Ms = Weight of sample.

2.4.3 Fat Content

Total fat content was determined by continuous lipid extraction of 2.00 g of homogenized samples in a Soxhlet apparatus for 5 h, using petroleum ether as the extraction solvent [11].

2.4.4 Total Protein

Protein content was determined in triplicate by analyzing total nitrogen using a Thermo Scientific Flash Smart™ Elemental Analyzer (Thermo Fisher Scientific, Waltham, MA, USA) based on the Dumas combustion method. Approximately 2–3 mg of sample was combusted at high temperature in an oxygen-rich atmosphere, and the resulting gases were passed through oxidation and reduction columns, where nitrogen was quantitatively converted to N_2. Detection was carried out with a thermal conductivity detector, and protein content was calculated from the nitrogen concentration using a conversion factor of 6.25, which is widely applied for diverse sample matrices [13].

2.4.5 Total Carbohydrate

Total carbohydrate content was estimated using the arithmetic difference method, whereby the proximate composition values of the other measured components were subtracted from 100, as shown in the Eqn. 3.

$$\% \text{ Carbohydrate } = 100 - (\% \text{ moisture } + \% \text{ fat } + \% \text{ protein } + \% \text{ ash }) \quad (3)$$

2.5 Fourier-Transform Infrared (FTIR)

FTIR spectroscopy coupled with attenuated total reflectance (ATR) was employed to analyze dried DDGS Protein and SPI samples using a Thermo Scientific Nicolet 8700 spectrometer (Waltham, MA, USA). Measurements were performed on a diamond crystal plate at a spectral resolution of 4 cm^{-1}, with spectra collected over the range of 4000–600 cm^{-1} by averaging 64 scans per sample. The amide II region (1500–1600 cm^{-1}) was extracted and processed in OriginPro 2024b (Learning Edition; OriginLab Corporation, Northampton, MA, USA). To enhance peak resolution, second-derivative spectra were calculated, followed by spectral deconvolution using the Peak Analyzer tool with a Gaussian fitting model to resolve overlapping peaks. The relative proportions of protein secondary structures were estimated by integrating the areas under the deconvoluted peaks. All deconvolution analyses were performed in triplicate.

2.6 Sodium Dodecyl Sulfate–Polyacrylamide Gel Electrophoresis (SDS-PAGE)

Sodium dodecyl sulfate–polyacrylamide gel electrophoresis (SDS-PAGE) was performed using Mini-PROTEAN precast gels (Bio-Rad Laboratories, Hercules, CA, USA). Molecular weight estimation was carried out with Bio-Rad Precision Plus Protein Standards (10–250 kDa). Samples were prepared by mixing with an equal volume of Laemmli sample buffer and electrophoresed in Mini-PROTEAN cells at 150 V for 40 min, or until the tracking dye reached the bottom of the gel. Following electrophoresis, the gels were stained with Coomassie Brilliant Blue R-250 and destained with multiple changes of distilled water until protein bands were clearly resolved.

2.7 Differential Scanning Calorimetry (DSC)

The thermal behavior of SPI and DDGS protein was assessed using a TA DSC 2500 differential scanning calorimeter (TA Instruments, New Castle, DE, USA), following the protocol of Das *et al.* [14] with minor modifications. Approximately 6–8 mg of protein sample was accurately weighed into an aluminum pan using a Mettler Toledo Analytical Plus precision balance (Mettler-Toledo, LLC, Polaris Parkway, Columbus, OH, USA). The pan's initial weight was recorded both before and after sample addition. Each pan was hermetically sealed and subjected to a thermal scan from 20 °C to 130 °C at a heating rate of 10 °C/min. A hermetically sealed empty pan served as the reference. Key thermal parameters, including onset temperature, peak temperature, and transition enthalpy, were extracted from the DSC thermograms using TRIOS software (version V5.6.0.87, TA Instruments, New Castle, DE, USA).

2.8 Thermogravimetric Analysis (TGA)

The thermal stability of the samples was evaluated using a TGA 550 thermogravimetric analyzer (TA Instruments, New Castle, DE, USA). Aluminum pans were pretared for 10 min prior to sample loading. The film samples were heated from 20 °C to 800 °C at a heating rate of

20 °C/min under a nitrogen flow of 60 mL/min. The sample weight percentage was recorded as a function of temperature, and the resulting thermograms were analyzed using TRIOS software (v5.1.1.46572, TA Instruments, New Castle, DE, USA).

2.9 Amino Acid Profiling

Comprehensive amino acid profiles were obtained by submitting samples to a commercial analytical laboratory (University of Missouri, Columbia, MO, USA), where analyses were conducted in accordance with AOAC Official Method 982.30 E(a,b,c), ch. 45.3.05 [15]. Amino acids were quantified by postcolumn ninhydrin derivatization using norleucine as an internal standard on a Hitachi Amino Acid Analyzer (Model L8900; Hitachi High Technologies America Inc., Pleasanton, CA, USA). Before analysis, samples were hydrolyzed in 6 N HCl at 110 °C for 24 h. Methionine and cysteine were quantified as methionine sulfone and cysteic acid, respectively, following cold performic acid oxidation overnight prior to acid hydrolysis. Tryptophan was determined separately after alkaline hydrolysis at 110 °C for 22 h.

2.10 Statistical Analysis

The experimental data obtained were analyzed using Minitab software (version 22.2.1, https://www.minitab.com/en-us/) to perform multiple regression analysis. The obtained data was fitted by an empirical linear and second-order polynomial (pure quadratic) model. Minitab statistical software was also used for surface plotting, data analysis, optimization, and experimental design. For the yield, the following model was suggested Eqn. 4.

$$\begin{aligned} Y = {} & b_0 + b_1X_1 + b_2X_2 + b_3X_3 + b_4X_4 + b_{11}X_1^2 \\ & + b_{22}X_2^2 + b_{33}X_3^2 + b_{44}X_4^2 + b_{12}X_1X_2 + b_{13}X_1X_3 \\ & + b_{14}X_1X_4 + b_{23}X_2X_3 + b_{24}X_2X_4 + b_{34}X_3X_4 \end{aligned} \quad (4)$$

where Y represents the response (protein yield); b_0 is the central value of the fixed response; b_1, b_2, b_3, and b_4 are the linear terms' coefficients; b_{11}, b_{22}, b_{33}, and b_{44} are the quadratic terms' coefficients, whereas b_{12}, b_{13}, b_{14}, b_{23}, b_{24}, and b_{34} are the cross-product coefficients.

3. Results and Discussion

3.1 Response Surface Methodology

Protein extraction yield, Y_1, and protein concentration, Y_2, were measured in 31 experimental runs with four independent variables, X_1, X_2, X_3, and X_4 (Minitab software, version 22.2.1). The results are summarized in Table 2. The highest protein extraction yield, Y_1, was 23.97% with variable conditions at X_1, X_2, X_3, X_4 = (–1, 1, 1, 1). The protein concentration, Y_2, under this condition was 724.14 mg/mL. On the contrary, with X_1, X_2, X_3, X_4 = 0, 2, 0, and 0, respectively, the highest protein concentration recorded was 941.21 mg/mL (Y_2), and the corresponding protein extraction efficiency, Y_1, was 21.71%. These results illustrate the interaction between process conditions and performance measures in the development of protocols for optimal protein extraction.

3.1.1 Regression Model for Protein Yield

The data presented in Table 1 were analyzed (Minitab software, version 22.2.1) using multiple regression to evaluate the effects of linear, quadratic, and interaction terms of the factors on protein extraction yield (Y_1) from DDGS, with results summarized in Table 3. The overall model was statistically significant (F = 10.93, $p < 0.001$), with the predictors explaining 90.52% of the total variation (Adj SS = 996.72). Examination of individual and combined term contributions provides insight into the factors and interactions that play a key role in protein extraction.

The regression model equation for protein extraction yield (Y_1) is shown in Eqn. 5 as follows:

$$\begin{aligned} \text{Yield } (Y_1) = {} & -48.2 + 1.433X_1 + 45.41X_2 + 2.416X_3 \\ & -0.73X_4 - 0.00609X_1^2 - 16.51X_2^2 - 0.0311X_3^2 + 0.35X_4^2 \\ & -0.3742X_1X_2 - 0.04246X_1X_3 - 0.0912X_1X_4 \\ & -0.359X_2X_3 + 4.54X_2X_4 + 0.314X_3X_4 \end{aligned} \quad (5)$$

The linear terms of the model had a very significant effect on Y_1 (F = 17.97, $p < 0.001$). Among them, NaOH concentration (F = 48.77, $p < 0.001$) and the solid-to-liquid ratio (F = 20.42, $p < 0.001$) were the most critical, indicating that these two factors are very crucial for the optimization of protein extraction. The quadratic terms are significant, F = 7.86, $p = 0.001$, which means nonlinear relationships between some factors and the response do exist. Specifically, the quadratic effects of NaOH concentration F = 14.95, $p = 0.001$ and ethanol concentration F = 8.08, $p = 0.012$ were statistically significant, emphasizing the curvature effects of these parameters. However, the quadratic terms for solid to liquid ratio (F = 2.60, $p = 0.126$) and time (F = 0.03, $p = 0.858$) were not significant. The high R^2 agrees with the significant F-value of 10.93 at $p < 0.001$ as presented in the ANOVA table, indicating that the model effectively captured important relationships. Most of the variance in Y_1 is well described by NaOH concentration, solid to liquid ratio, and their interactions with ethanol concentration. However, the moderate R^2 pred and the significant lack-of-fit (F = 4.45, $p = 0.040$) suggest that the model may not fully capture some underlying complexities in the system. To check the model's adequacy, the error test of lack-of-fit was carried out. The test is meant to check for any inaccuracies due to some defect in the model structure [16]. In cases where the *p*-value of the lack-of-fit F-statistic is above the level of significance or confidence interval, the lack of fit will be regarded as insignificant, hence the model is adequate for explaining the data. The absence of an ap-

Table 2. Experimental coded values, actual values of central composite design and responses of protein yield and protein concentration.

Coded variables					Uncoded variables				Responses	
Runs	X_1	X_2	X_3	X_4	Ethanol (X_1) (%)	NaOH (X_2) (Molar)	Solid to liquid ratio (X_3)	Time (X_4) (hr.)	Y_1 (%)	Y_2 (mg/mL)
1	1	–1	–1	1	75	0.050	5	2.0	11.31	266.86
2	0	0	2	0	60	0.525	15	1.5	10.33	611.07
3	–1	–1	–1	1	45	0.050	5	2.0	2.31	248.79
4	0	0	0	0	60	0.525	10	1.5	15.63	513.43
5	–1	–1	1	1	45	0.050	15	2.0	5.44	238.93
6	–1	1	–1	–1	45	1.000	5	1.0	14.44	441.71
7	0	–2	0	0	60	0.050	10	1.5	7.37	262.79
8	2	0	0	0	90	0.525	10	1.5	10.00	360.50
9	0	0	0	0	60	0.525	10	1.5	14.81	567.93
10	1	–1	–1	–1	75	0.050	5	1.0	14.25	254.07
11	1	1	1	–1	75	1.000	15	1.0	2.79	683.29
12	0	0	0	0	60	0.525	10	1.5	16.56	651.07
13	0	0	0	0	60	0.525	10	1.5	18.38	596.64
14	0	0	0	–2	60	0.525	10	0.5	17.13	606.64
15	0	0	0	0	60	0.525	10	1.5	15.28	531.00
16	0	0	0	0	60	0.525	10	1.5	15.16	564.93
17	–1	1	1	–1	45	1.000	15	1.0	15.56	860.86
18	0	2	0	0	60	1.000	10	1.5	23.97	724.14
19	–1	1	1	1	45	1.000	15	2.0	21.71	941.21
20	1	1	–1	–1	75	1.000	5	1.0	20.06	515.64
21	1	1	1	1	75	1.000	15	2.0	4.02	595.71
22	0	0	0	0	60	0.525	10	1.5	18.03	597.57
23	1	–1	1	1	75	0.050	15	2.0	5.15	309.14
24	–1	1	–1	1	45	1.000	5	2.0	19.56	524.00
25	0	0	–2	0	60	0.525	5	1.5	18.38	520.14
26	0	0	0	2	60	0.525	10	2.0	18.50	498.79
27	–1	–1	–1	–1	45	0.050	5	1.0	6.91	233.14
28	1	–1	1	–1	75	0.050	15	1.0	5.04	315.57
29	–1	–1	1	–1	45	0.050	15	1.0	5.77	263.93
30	1	1	–1	1	75	1.000	5	2.0	17.06	448.79
31	–2	0	0	0	30	0.525	10	1.5	13.97	640.14

propriate fit is indicated in a case where the F-statistic related to a lack-of-fit shows a significant result, meaning a smaller *p*-value than the selected significance level [17].

3.1.2 Regression Model for Protein Concentration

The data presented in Table 4 were analyzed using multiple regression to assess the effects of linear, quadratic, and interaction terms of the factors on protein concentration (Y_2) in DDGS. The resulting regression equation for protein concentration (Y_2) is provided in Eqn. 6 below.

$$\begin{aligned}\text{Protein Concentration } (Y_2) = {} & -614 + 18.80X_1 + \\ & 935X_2 + 26.1X_3 + 238X_4 - 0.0899X_1^2 - 436X_2^2 \\ & -0.156X_3^2 - 28.5X_4^2 - 6.01X_1X_2 - 0.366X_1X_3 \\ & -2.51X_1X_4 + 27.01X_2X_3 + 3.0X_2X_4 - 2.06X_3X_4\end{aligned} \quad (6)$$

The results of ANOVA (Table 4) present the significance of the regression model and its components toward explaining the variation in the response variable, Y_2. The regression model is highly significant with F = 13.53, $p < 0.001$, and explains 92.21% of the total variability in the response, R^2 = 92.21%. An adjusted R^2 of 85.40% indicated that the model was good even after accounting for the number of predictors. The low standard error, S = 71.1162, suggests good precision in the predictions. However, the predicted R^2 (54.02%) indicates that the model's ability to generalize to new data is moderate, suggesting potential overfitting or omitted variables.

The linear terms had an overall significant contribution on the response (F = 36.90, $p < 0.001$). Of all the variables, NaOH concentration, Solid-to-liquid ratio and Ethanol concentration were significant. Time (F = 0.37, p = 0.554) was not significant, therefore not contributing meaningfully alone to the response. The quadratic terms were

Table 3. Analysis of variance summary for the model interactions for protein yield, Y_1.

Source	DF	Adj SS	Adj MS	F-Value	*p*-value
Model	14	996.72	71.194	10.93	0.000
Linear	4	468.21	117.052	17.97	0.000
Ethanol (X_1)	1	16.58	16.580	2.54	0.130
NaOH (X_2)	1	317.73	317.730	48.77	0.000
Solid to liquid ratio (X_3)	1	133.06	133.059	20.42	0.000
Time (X_4)	1	0.84	0.840	0.13	0.724
Square	4	204.94	51.236	7.86	0.001
Ethanol×Ethanol (X_1^2)	1	52.65	52.650	8.08	0.012
NaOH×NaOH (X_2^2)	1	97.38	97.375	14.95	0.001
Solid to liquid ratio×Solid to liquid ratio (X_3^2)	1	16.94	16.944	2.60	0.126
Time×Time (X_4^2)	1	0.22	0.217	0.03	0.858
2-Way Interaction	6	323.57	53.928	8.28	0.000
Ethanol×NaOH (X_1X_2)	1	113.72	113.722	17.45	0.001
Ethanol×Solid to liquid ratio (X_1X_3)	1	162.23	162.231	24.90	0.000
Ethanol×Time (X_1X_4)	1	7.49	7.491	1.15	0.300
NaOH×Solid to liquid ratio (X_2X_3)	1	11.66	11.656	1.79	0.200
NaOH×Time (X_2X_4)	1	18.62	18.620	2.86	0.110
Solid to liquid ratio×Time (X_3X_4)	1	9.85	9.847	1.51	0.237
Error	16	104.25	6.515		
Lack-of-Fit	10	91.87	9.187	4.45	0.040
Pure Error	6	12.38	2.063		
Total	30	1100.97			

R-sq(pred) 64.92%, R-sq(adj) 82.25%. DF, Degree of Freedom; SS, Sum of Square; MS, Mean Square.

Table 4. Analysis of variance summary for the model interactions for protein yield, Y_2.

Source	DF	Adj SS	Adj MS	F-value	*p*-value
Model	14	958,030	68,431	13.53	0.000
Linear	4	746,391	186,598	36.90	0.000
Ethanol	1	35,481	35,481	7.02	0.018
NaOH	1	620,551	620,551	122.70	0.000
Solid to liquid ratio	1	88,513	88,513	17.50	0.001
Time	1	1846	1846	0.37	0.554
Square	4	98,324	24,581	4.86	0.009
Ethanol×Ethanol	1	11,483	11,483	2.27	0.151
NaOH×NaOH	1	67,872	67,872	13.42	0.002
Solid to liquid ratio×Solid to liquid ratio	1	427	427	0.08	0.775
Time×Time	1	1425	1425	0.28	0.603
2-Way Interaction	6	113,315	18,886	3.73	0.016
Ethanol×NaOH	1	29,345	29,345	5.80	0.028
Ethanol×Solid to liquid ratio	1	12,041	12,041	2.38	0.142
Ethanol×Time	1	5676	5676	1.12	0.305
NaOH×Solid to liquid ratio	1	65,820	65,820	13.01	0.002
NaOH×Time	1	8	8	0.00	0.969
Solid to liquid ratio×Time	1	425	425	0.08	0.776
Error	16	80,920	5058		
Lack-of-Fit	10	68,278	6828	3.24	0.082
Pure Error	6	12,642	2107		
Total	30	1,038,950			

R-sq(pred) 64.92%, R-sq(adj) 82.25%.

collectively significant (F = 4.86, $p = 0.009$), which showed that the response surface had a curvature. The quadratic effect of NaOH concentration (F = 13.42, $p = 0.002$) was significant, showing a non-linear relationship, while other

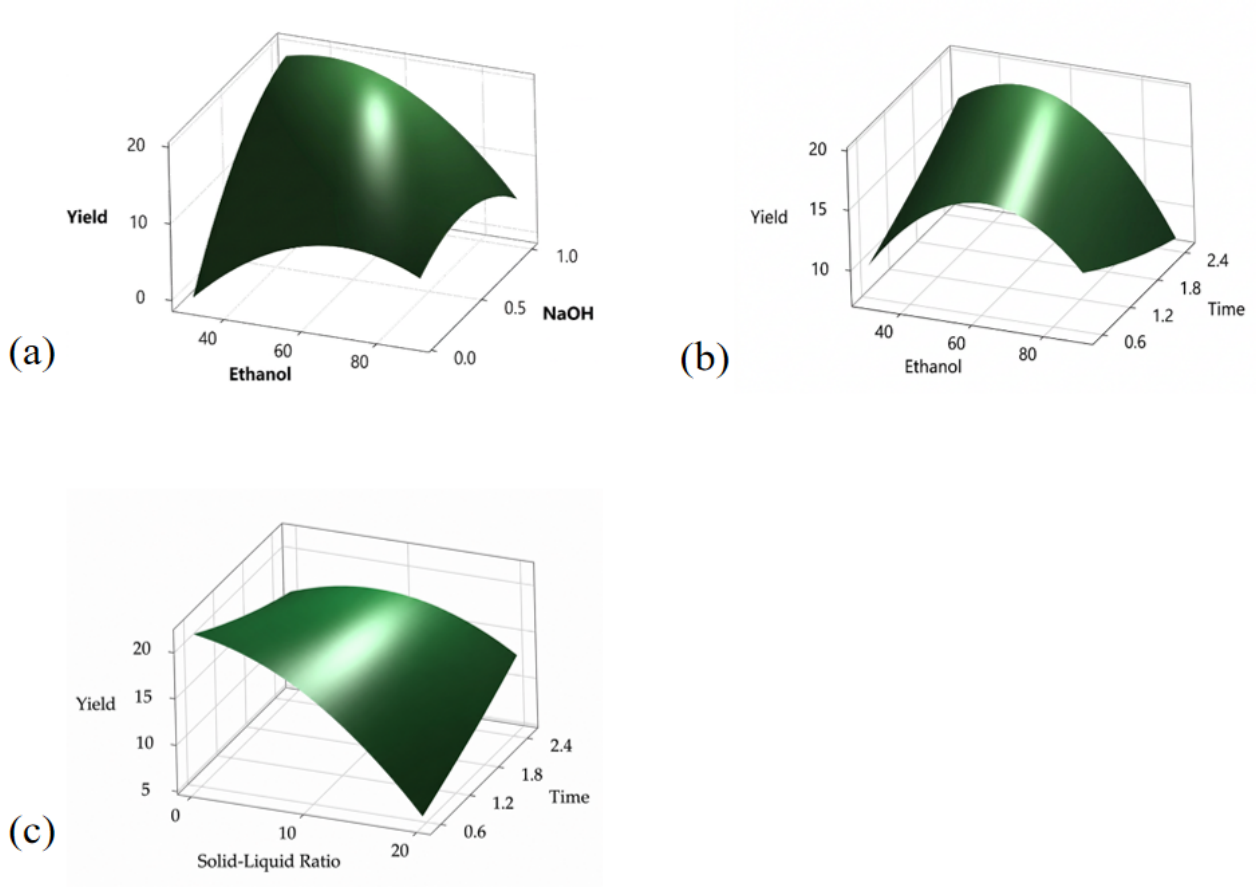

Fig. 1. Surface plot of protein yield. Surface plot of protein yield vs ethanol and NaOH (a), Surface plot of protein yield vs ethanol and time (b), Surface plot of protein yield vs solid to liquid ratio and time (c).

quadratic terms involving ethanol concentration, solid to liquid ratio, and time were not significant. The two-way interaction terms were jointly significant, $F = 3.73$, $p = 0.016$, whereas interactions involving time, for instance, were not significant, thus limited synergistic effects involving time. The lack-of-fit test was not significant ($F = 3.24$, $p = 0.082$), indicating that the model provides an adequate fit and that there is no substantial deviation between the predicted and experimental data [16]. The low pure error (SS = 12,642; MS = 2107) further confirms the precision and reliability of the experimental results.

3.2 Surface Plots for Protein Yield

Ideal conditions for this study were selected using surface plots. Predicting the response variables and changing the other two independent variables aided in determining the optimal yield at any given point. Fig. 1a shows that the interaction of ethanol and NaOH concentrations had a significant effect on protein extraction yield, with a maximum yield of about 23% when NaOH and ethanol were optimized at 1 molar and 60%, respectively. Further increases in NaOH concentration beyond the optimum reduced protein yield, probably because of protein denaturation by high levels of NaOH in the DDGS matrix. Specifically, the interaction between ethanol concentration and extraction time resulted in the maximum protein yield at 60% ethanol and an extraction time of 2 h (Fig. 1b). Fig. 1c further present that with increased extraction time, an increase in protein yield is obtained. Additionally, the interaction between extraction time and sample-to-solvent ratio indicated that the highest protein yield was achieved at a solid-to-solvent ratio of 1:10.

However, NaOH concentration and extraction time must be optimized to avoid detrimental effects on the nutritional value of proteins extracted, as observed earlier by other researchers too [6]. Besides, further increasing the extraction time out of the studied range resulted in a negligible effect on protein recovery, indicating a kind of saturation phenomena under the given experimental conditions.

An optimization study on protein extraction from soybean was reported [9], in which four independent variables—temperature (25–85 °C), NH_4OH concentration (0.5–1.5%), extraction time (6–24 h), and solvent ratio (1:5–1:20 w/v)—were evaluated to improve extraction efficiency. RSM combined with a central composite design (CCD) was employed, with amine concentration and protein yield as the response variables. Optimal conditions for maximum protein yield (65.66%) with minimal amine con-

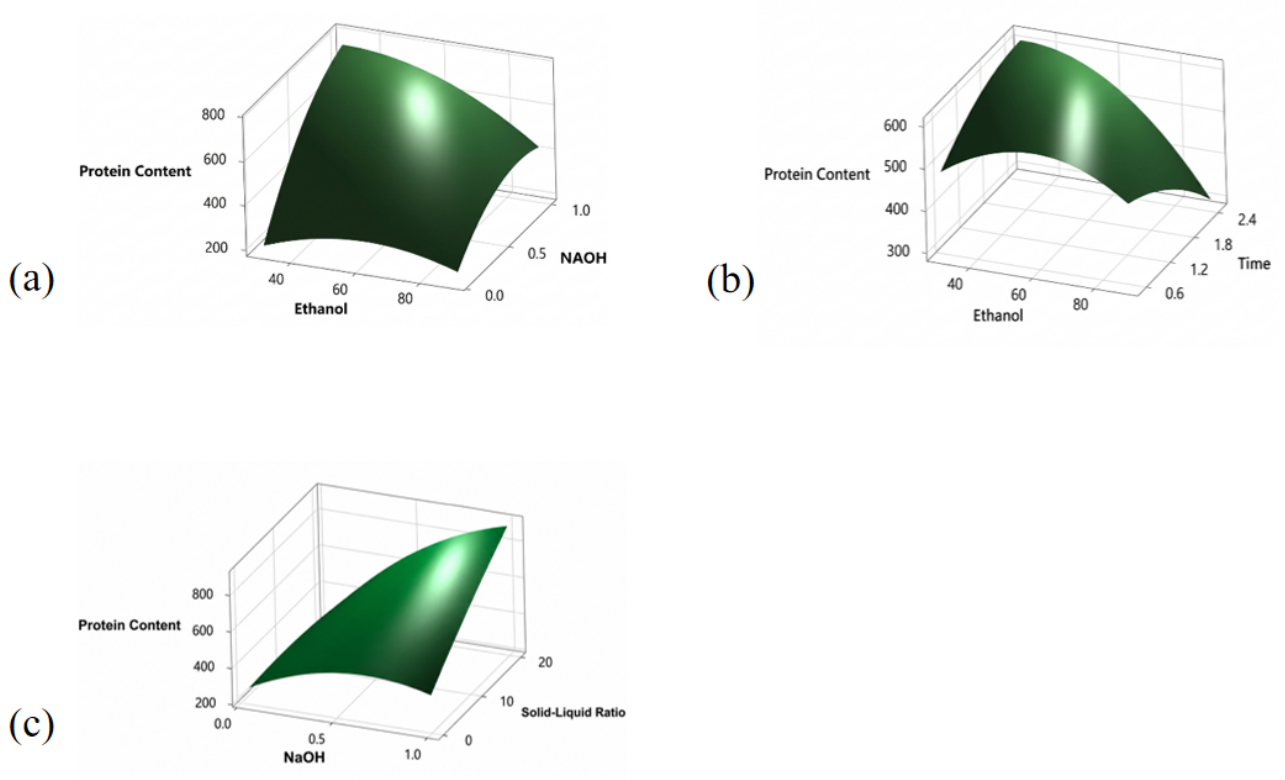

Fig. 2. Surface plot of protein content. Surface plot of protein content vs ethanol and NaOH (a), Surface plot of protein content vs ethanol and time (b), Surface plot of protein content vs solid to liquid ratio and time (c).

tent (0.14 mM) were identified as 52.5 °C, 0.5% NH_4OH, a 1:10 (w/v) solvent ratio, and a 12-hour extraction period. Similarly, a separate study [7] optimized protein extraction from DDGS using three key process variables: alkali concentration, extraction time, and solid-to-liquid ratio. The RSM-based model predicted the optimal conditions to be a solid-to-liquid ratio of 1:37 (g:mL), an extraction time of 2.3 h, and an alkali concentration of 0.626 mol/L.

Fig. 2a shows that the interaction of ethanol and NaOH concentrations had a significant effect on protein concentration, with a maximum value of 941.21 mg/mL when NaOH and ethanol were optimized at 1 molar and 45%, respectively. Increasing NaOH up to a certain point improves protein extraction by breaking down protein structures and increasing solubility. Excessive NaOH may lead to protein denaturation, reducing the extraction yield, which might explain why the surface curve does not increase indefinitely. Too much ethanol could cause protein aggregation while too little may lead to poor extraction.

The surface curve indicates a nonlinear relationship among ethanol, time, and protein content (Fig. 2b). Protein content rises with an increase in ethanol concentration, going to a peak before dropping at higher concentrations of ethanol. Protein content is affected by extraction time positively but, beyond a certain point, increased exposure leads to a decrease or plateau in protein content. In Fig. 2c the increase in protein content starts to flatten at the uppermost NaOH and solid to liquid ratio levels. This may indicate there is an optimum range above which further increases will not make any discernible improvement in protein content. An intermediate solid to liquid ratio offers adequate solvent for the dissolution of proteins while maintaining solution concentration, i.e., 1:10. Excessively high ratio might decrease solvent efficacy.

Another study reported [18] where temperature, alkaline solution, and extraction time were optimized for SPI extraction using a Box–Behnken design and response surface analysis. 93.15% of the variability was explained by a second-order polynomial model that suited the findings well. The ideal parameters were 44.7 minutes, 70 °C, and an alkaline solution with a pH of 12.68. Response surface methodology and factorial design were used to maximize the extraction of proteins from goat meat [19]. Temperature, extraction period, extractor volume, and extractor concentration were the factors under investigation. The ideal parameters were 3.5 mL extractor volume, 10 min extraction duration, 44 °C temperature, and 0.05 mol/L extractor concentration. Using the optimized extraction approach, a protein content of 19.3 g/100 g was achieved, which is higher than values previously reported in the literature. In a study [20], response surface methodology was applied to evaluate the effects of sonication amplitude, extraction time, and solid-to-liquid ratio on protein yield from rice bran. Protein yield during ultrasound-assisted ex-

Table 5. Shows the proximate analysis of DDGS, DDGS protein and SPI.

Proximate analysis			
	DDGS	DDGS Protein	SPI
Crude protein	24.94 ± 0.13	65.21 ± 0.72	71.46 ± 0.36
Fat	4.73 ± 0.03	12.24 ± 0.25	12.00 ± 0.02
Moisture content	15.67 ± 0.02	2.33 ± 0.02	9.00 ± 0.01
Carbohydrate	45.00 ± 0.54	17.22 ± 0.24	5.88 ± 0.13
Ash	9.67 ± 0.01	3.00 ± 0.03	1.67 ± 0.01

traction (UAE) was strongly influenced by both sonication amplitude and extraction duration. The optimal extraction conditions were determined to be a solid-to-liquid ratio of 0.99 g/10 mL, an extraction time of 18 min, and a sonication amplitude of 76%. In the present study, optimum parameters of protein extraction from DDGS were determined at that point where concentration of protein was highest, indicating the maximum protein yield can be achieved; hence, they were somewhat different from the previously reported values.

Validation of Optimized Conditions

The optimal conditions identified in the previous study (2 h extraction time, a solid-to-solvent ratio of 1:10 w/v, NaOH concentration of 1 M, and ethanol concentration of 60%) were employed to replicate the experiment. The protein yield predicted by the RSM regression model was 23.97%, while the experimentally obtained yield under these conditions was 23%. This close agreement confirms the validity of the regression model.

3.3 Characterization

3.3.1 Proximate Composition Analysis

The proximate composition of DDGS, DDGS protein, and Soy Protein Isolate (SPI) is presented in Table 5. The data indicates distinct compositional variations among the samples, reflecting the impact of protein isolation and difference in processing conditions on the quality and structure of the product.

The efficiency of the protein extraction procedure was demonstrated by the significant increase in crude protein content from 24.94% in DDGS to 65.21% in DDGS protein isolate. This enrichment is in line with earlier research showing that, depending on the extraction technique employed, the protein content of DDGS isolates varied from 60% to 70% [21]. On the other hand, SPI showed the highest protein concentration at 71.46%, which is consistent with the standard SPI values (70–90%) that have been documented in the literature [22]. This suggests that SPI is still a standard for protein purity.

The fat content in the DDGS protein isolate was 12.24%, significantly higher than in the raw DDGS (4.73%). This may be attributed to concentration effects during protein extraction or co-extraction of lipids [23]. Notably, the fat content in SPI was slightly lower (12.00%), which supports the idea that plant protein isolates can retain moderate lipid fractions, especially when not subjected to complete defatting.

Moisture content in DDGS was recorded at 15.67%, which sharply dropped to 2.33% in DDGS protein and 9.00% in SPI. The low moisture in DDGS protein indicates successful dehydration during processing, which is crucial for storage stability. Moisture levels below 10% are generally considered desirable to inhibit microbial activity [24]. The amount of carbohydrates in the DDGS protein reduced from 45.00% to 17.22%, suggesting that fiber and soluble sugars were significantly eliminated during protein enrichment. The lowest percentage of carbohydrates (5.88%) was found in SPI. Lastly, the ash concentration dropped from 9.67% in DDGS to 3.00% in DDGS protein, indicating that the mineral content was successfully removed during isolation. At 1.67%, SPI had the lowest ash value, which is typical of highly refined protein concentrates.

3.3.2 FTIR

When DDGS protein and SPI were analyzed using FTIR, their infrared reflectance across various wavenumbers reveals differing molecular compositions (Fig. 3). The contrasts between these two protein sources are highlighted by the spectra, which show distinctive functional groups linked to carbohydrates, proteins, and lipids. Around 3200–3500 cm^{-1}, a wide absorption was seen, which is indicative of hydroxyl (-OH) and amide (-NH) groups and correlates to O–H and N–H stretching vibrations [25,26]. In this area, the SPI sample shows more absorption, indicating a greater concentration of amide A structures, which are crucial protein constituents. Furthermore, the region between 2900 and 3000 cm^{-1}, which is ascribed to C-H stretching vibrations, exhibits a marginally higher intensity in DDGS, suggesting a higher concentration of residual lipids or carbohydrates.

The better protein purity and distinct secondary structure of SPI are confirmed by the more prominent amide I (~1650 cm^{-1}) and amide II (~1550 cm^{-1}) regions, which are linked to C=O stretching and N-H bending vibrations, respectively [27]. On the other hand, DDGS protein exhibits more complex characteristics, which are indicative of its larger fiber and carbohydrate content, in the 900–1200 cm^{-1} area, which corresponds to C–O, C–C, and C–H stretching in polysaccharides and lipids.

Phosphate groups (PO_4^{3-}) typically exhibit characteristic absorption bands in the range of 1200–900 cm^{-1}, primarily due to P=O stretching, P-O-C, and P-OH vibrations [28]. For SPI: The phosphate absorption appears around 1080–1050 cm^{-1}, which is characteristic of P=O stretching in phosphoproteins and phospholipids. For DDGS protein: The phosphate peak is more prominent around 1060–1020 cm^{-1}, likely due to phosphate groups present in nucleotides, phospholipids, or phosphorylated carbohydrates.

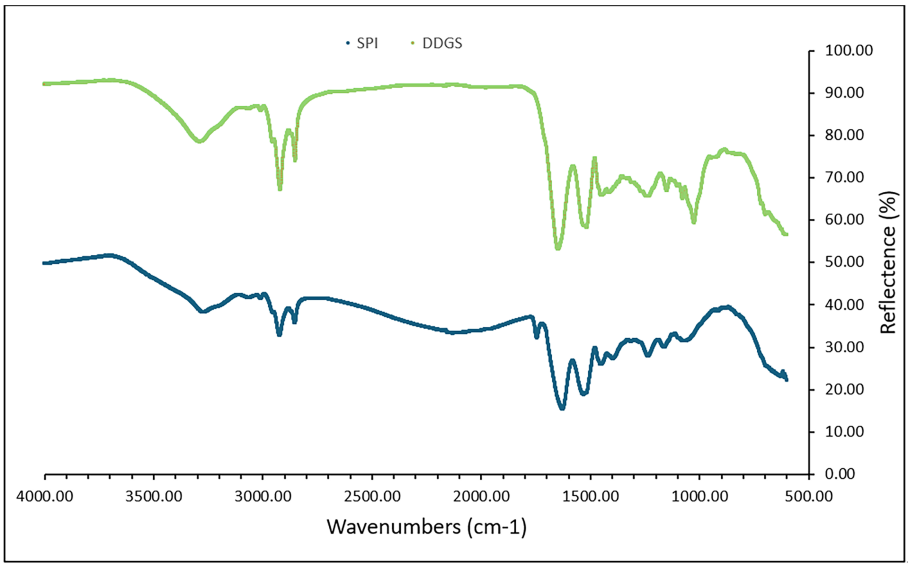

Fig. 3. FTIR spectra of SPI and DDGS protein. FTIR, fourier-transform infrared; SPI, soy protein isolate; DDGS, Distillers' Dried Grains with Solubles.

These spectrum differences show that while DDGS protein comprises a more varied biochemical matrix that includes proteins, fibers, and lipids, SPI is a more protein-dense matter with well-structured protein content.

3.3.3 TGA

The thermal degradation behaviors of SPI and DDGS were evaluated using thermogravimetric analysis, and the resulting weight-loss profiles are presented in Fig. 4. Both samples exhibited a typical two-stage degradation pattern characteristic of protein-rich biomaterials. The initial baseline region up to ~200 °C showed minimal mass loss (<5%), corresponding primarily to the release of bound moisture and loosely adsorbed volatiles [29]. The major decomposition stage for both SPI and DDGS occurred between approximately 250–420 °C, which is associated with cleavage of peptide bonds, breakdown of amino-acid side chains, and volatilization of degradation intermediates. However, clear differences in the onset and extent of thermal degradation were observed. SPI exhibited a higher decomposition onset at 281.02 °C, compared to the lower onset of 252.95 °C for DDGS. This suggests that SPI has stronger intramolecular connections and a more thermally stable primary protein structure, needing more thermal energy to start breakdown [30].

Conversely, the DDGS curve displayed a more gradual mass-loss transition, with its decomposition endset at 353.77 °C, while SPI continued degrading until a substantially higher endset of 412.52 °C. Higher structural homogeneity and more stable globular proteins (particularly glycinin and β-conglycinin), which disintegrate across a wider temperature range, are the reasons for this prolonged degradation in SPI. In contrast, the proteins in DDGS are thermally pre-treated and have already experienced partial denaturation during the drying, fermentation heating, and distillation stages of ethanol production. Although it lacks the longer-range stability of native SPI proteins, this partly unfolded, aggregated form is more vulnerable to early onset destruction.

3.3.4 DSC

The DSC thermograms of SPI and DDGS further elucidate their thermal transitions and complement the TGA findings Fig. 5. The SPI thermogram exhibited a single broad endothermic transition characterized by an onset temperature of 25.05 °C, a peak denaturation temperature of 89.23 °C, and a total enthalpy of 113.88 J/g. The relatively large enthalpy value indicates the presence of intact, highly ordered protein domains that require substantial energy input for disruption, consistent with the native structural integrity of SPI proteins [31].

In contrast, DDGS displayed an earlier and less intense endothermic event, with an onset at 25.07 °C, a peak at 48.93 °C, and a markedly lower enthalpy of 67.29 J/g. The presence of two midpoints at 44.05 °C suggests partial unfolding transitions that have become broadened due to structural heterogeneity introduced during DDGS processing [14]. The substantially reduced enthalpy implies that the DDGS protein matrix contains fewer ordered domains and weaker intermolecular bonding, consistent with prior exposure to high-temperature drying and fermentation-associated heating. These industrial processes partially denature and aggregate DDGS proteins, reducing the energy required to induce further thermal transitions.

SPI retains native globular protein structures, resulting in higher denaturation temperature and higher enthalpy, reflecting greater structural order and stronger stabilizing interactions (hydrogen bonding, hydrophobic packing).

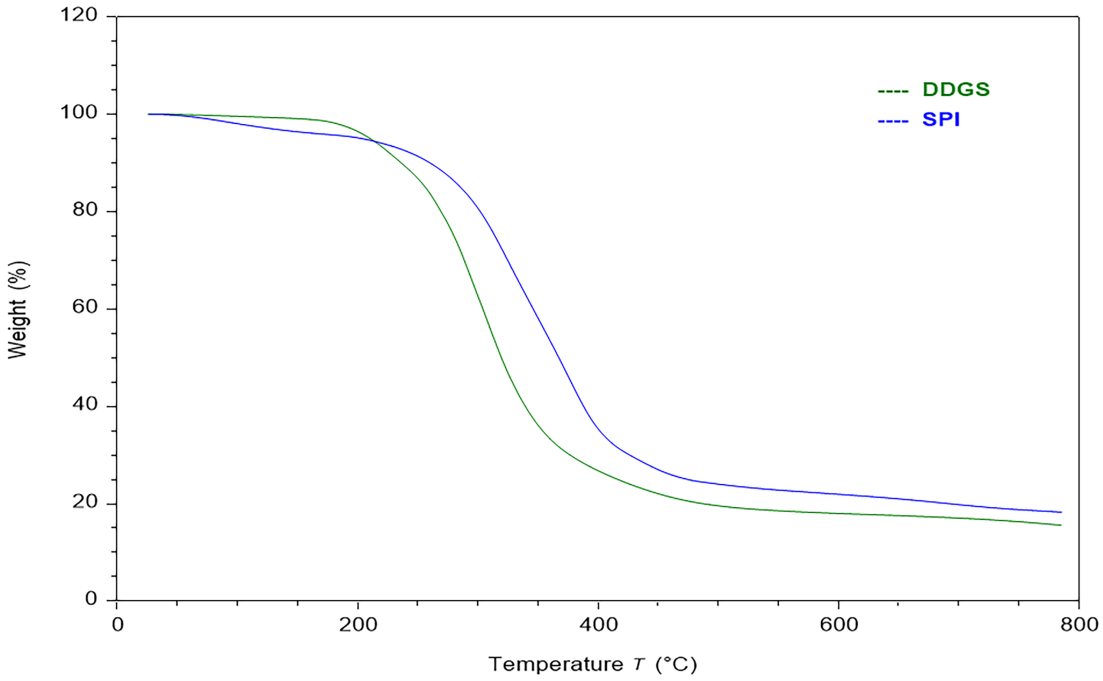

Fig. 4. TGA graph of weight loss with respect to temperature of protein isolates from SPI and DDGS protein. TGA, thermogravimetric analysis.

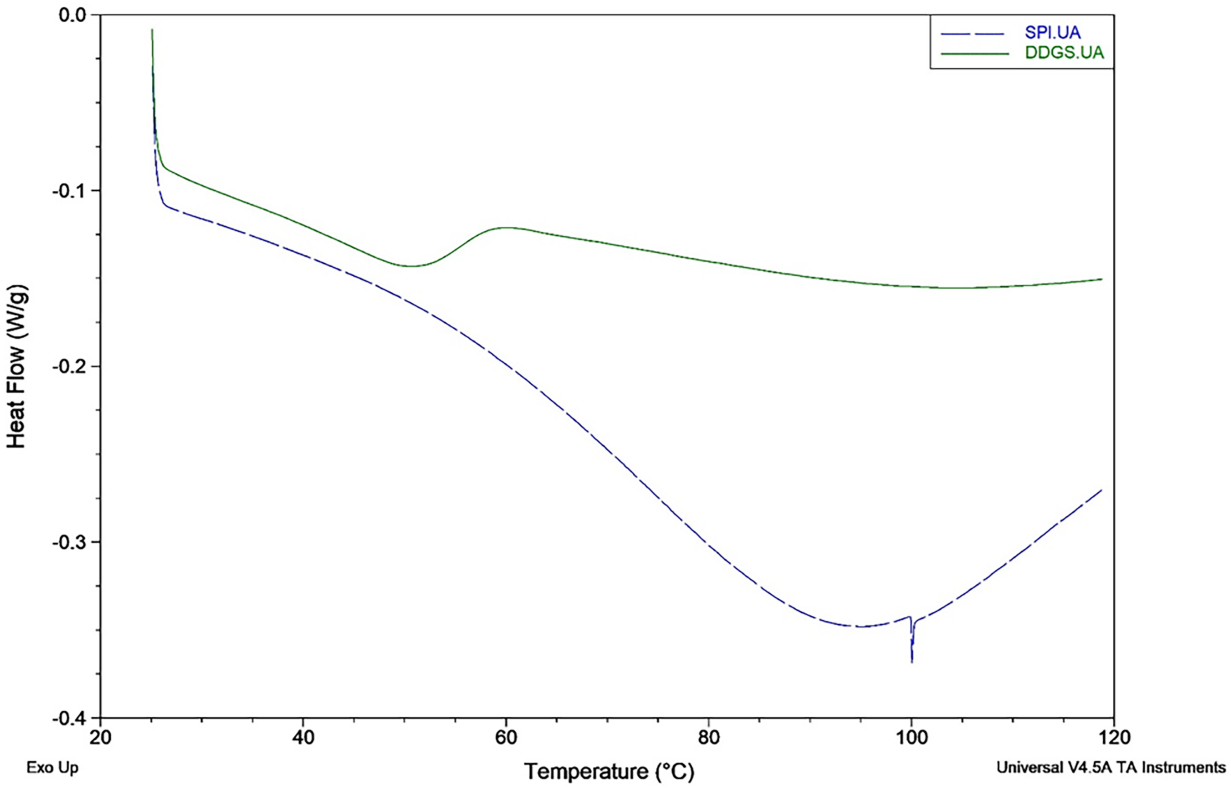

Fig. 5. DSC curves of protein isolates from SPI and DDGS protein. DSC, differential scanning calorimetry.

DDGS proteins exhibit lower thermal stability, as indicated by low peak temperature and reduced enthalpy, supporting the notion that processing-induced denaturation produces a less cohesive protein matrix. Importantly, while DDGS shows lower thermal stability (lower denaturation temperature and enthalpy), the broad, shallow nature of its endothermic curve corresponds well with TGA observations of gradual mass loss. This behavior represents thermal re-

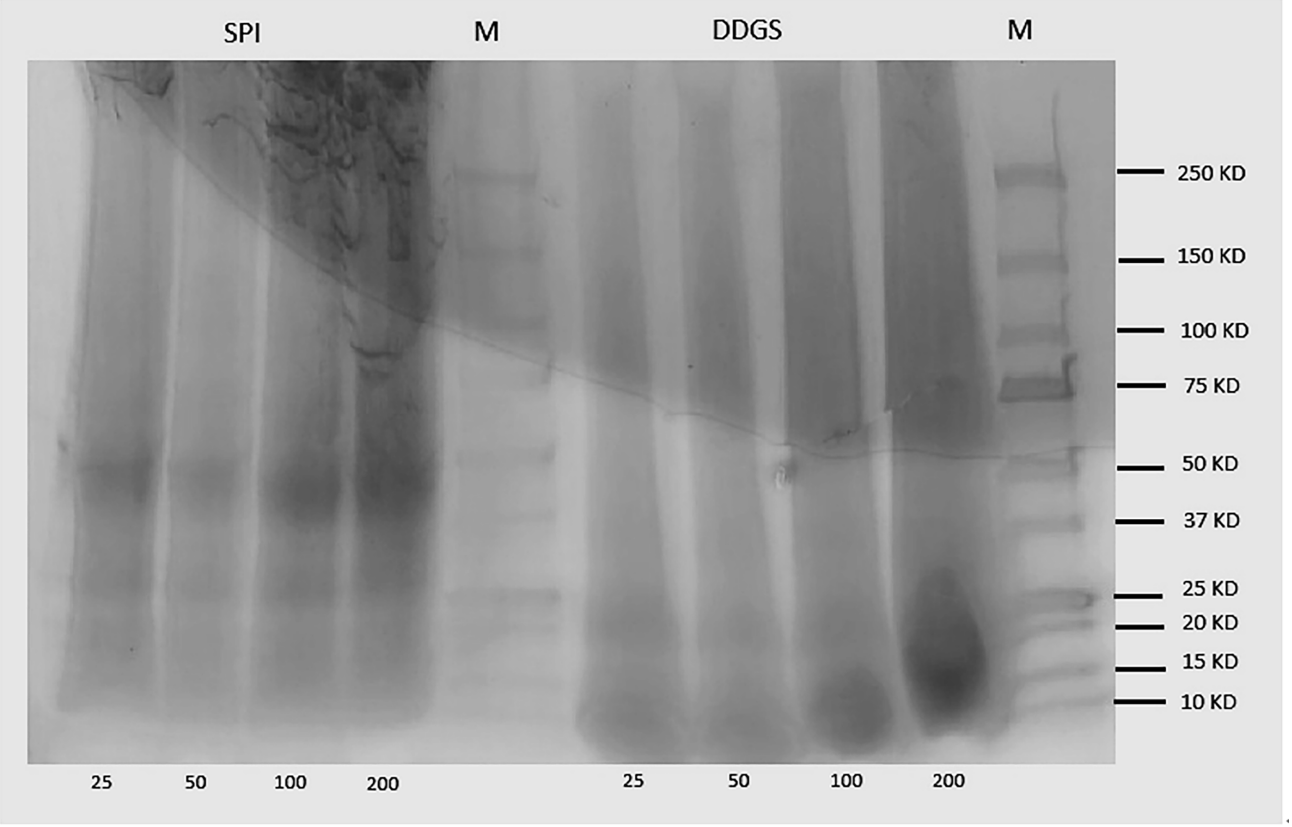

Fig. 6. Molecular weight distribution at different concentrations (25–200 mg/mL) of SPI and DDGS protein. M is the protein ladder.

sistance, meaning the material does not collapse sharply with heat but transitions gradually due to its already partially denatured and crosslinked structure from industrial processing.

3.3.5 SDS-PAGE

The protein molecular weight distribution in DDGS protein and SPI can be compared using the Sodium Dodecyl Sulfate-Polyacrylamide Gel Electrophoresis (SDS-PAGE) study. Protein fractions in the SPI and DDGS protein samples can be identified with respect to the molecular weight marker (M), which has reference bands with a molecular weight between 10 kDa and 250 kDa (Fig. 6). Different protein bands are evident in the SPI lanes, mostly in the 20–100 kDa range, however, some bands of higher molecular weight are barely perceptible. This implies the existence of globular proteins that are typical of soy protein, such as glycinin (70–80 kDa) and β-conglycinin (35–55 kDa) [32]. The distinct bands demonstrate the high protein integrity and purity of SPI by showing that it is composed of soluble and structural protein fractions.

On the other hand, the DDGS protein lanes show a fainter and more scattered banding pattern, with noticeable bands seen below 50 kDa, especially around 25 and 15 kDa. This implies that DDGS proteins are either smaller by nature or have been degraded during the processing of ethanol. Four closely spaced bands at roughly 21 kDa, 25 kDa, 27 kDa, and 37 kDa were shown when the composition of the extracted protein from DDGS. The main protein group in corn is the zein family, which these protein fractions most likely belong to. In addition to other lower molecular weight proteins, zeins are categorized as α-zeins, δ-zeins, γ-zeins, and β-zeins. They are made up of a variety of closely related polypeptides, such as α-zeins at 19 and 22 kDa, β-zeins at 14 kDa, δ-zeins at 10 kDa, and γ-zeins at 16 and 27 kDa [33]. It is possible that these lower-molecular-weight fractions were eliminated during the ethanol fermentation process because column 1 of the gel shows no proteins smaller than 10 kDa.

This could be because of denaturation, cross-linking, or interactions with fiber and carbohydrate components during fermentation and drying. Variations in protein quality, solubility, and extraction conditions are reflected in the clear disparities in protein molecular weight distribution between SPI and DDGS protein. While DDGS protein is made up of smaller protein fragments, most likely because of processing effects, SPI shows broader and more distinct protein bands, suggesting a structured protein profile with improved functional stability. Reduced structural integrity and solubility are suggested by the more fragmented form of DDGS proteins, which could have an impact on their digestibility and functional uses. While DDGS protein,

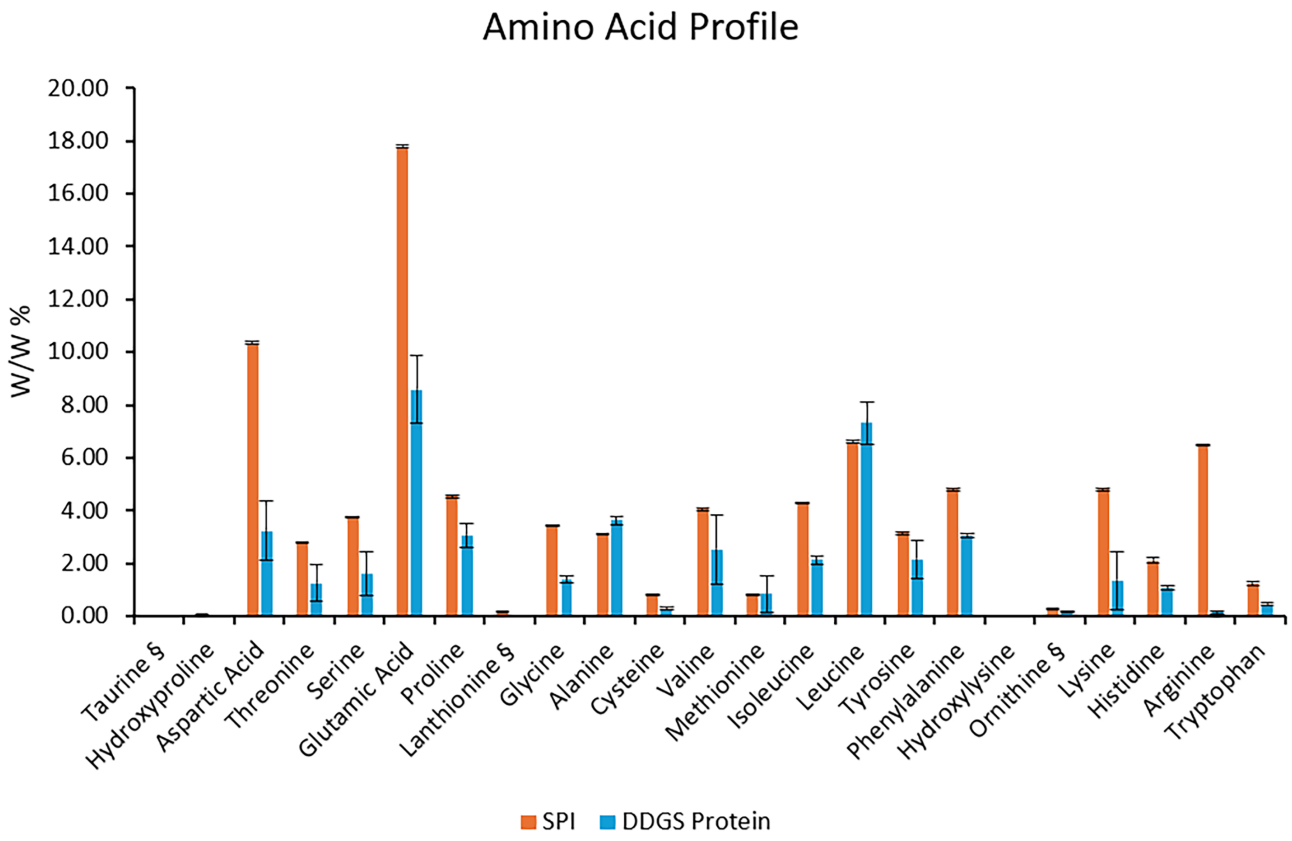

Fig. 7. Amino acid composition of DDGS protein and SPI.

with its lower molecular weight protein fractions, may be more suited for feed and enzymatic hydrolysis applications where smaller peptides are advantageous, SPI's intact protein structure makes it suitable for food and protein-based formulations. These findings have important industrial implications.

3.3.6 Amino Acid Profile

The amino acid profiles of SPI and DDGS protein are compared, revealing significant variations in their makeup and their uses (Fig. 7). SPI has a substantially greater total amino acid content (85.63 g/100 g) than DDGS protein (44.47 g/100 g), which is consistent with its higher crude protein concentration (89.04% vs. 44.25%) [34]. SPI's greater abundance of essential amino acids, including leucine, lysine, isoleucine, valine, and methionine, highlights its superior nutritional value. Higher concentrations of glutamic acid and aspartic acid, which are necessary for protein synthesis and metabolic processes, are also present in SPI. SPI's increased branched-chain amino acid (BCAA) content benefits muscle protein synthesis and makes it more appropriate for high-nutritional use. However, because of its affordability, accessibility, and sustainability, DDGS protein is still a good substitute protein source even with its decreased amino acid content. For ruminants, its high fiber content offers substantial digestion advantages, even though it is restrictive for monogastric animals. Furthermore, its remaining lipid content helps animal feed supplement with energy. Even though SPI provides higher-quality protein, DDGS protein is still a viable option for livestock nutrition, especially for ruminant diets, because of its practical advantages, affordability, and environmental sustainability, which make it a wise decision for both industrial and agricultural settings.

4. Limitations

This study has several limitations that should be considered when interpreting the findings. The optimization was conducted using DDGS obtained from a single ethanol plant and a single production batch, which limits the generalizability of the identified extraction conditions because DDGS composition can vary across feedstocks, processing conditions, and production facilities. The extraction temperature was fixed at 55 °C rather than included as an independent optimization factor, which may have constrained identification of a broader or more robust optimum because temperature strongly influences protein solubility, denaturation, and extraction behavior. Also, comparison with soy protein isolate was based on a single commercial SPI sample, so the observed differences should be interpreted cautiously and not assumed to represent all SPI products with differing sources or processing histories.

5. Conclusion

The study utilized response surface methodology to optimize the extraction of proteins from DDGS, achieving a protein yield of around 23% with specific parameters such as a 2-hour extraction time, a 1:10 solid-to-liquid ratio, 1 M NaOH, and 60% ethanol, which validated successfully through empirical testing. Chemical analyses showed significant enrichment of crude protein from 24.94% in raw DDGS to 65.21% in the isolate, alongside increased lipid content due to co-extraction, while moisture, carbohydrates, and ash contents decreased, indicating effective purification. Structural analysis via SDS-PAGE revealed that SPI maintained high structural integrity with characteristic intact globular protein bands, whereas DDGS proteins appeared fragmented with lower molecular weight bands, likely due to denaturation and interactions with fibers and carbohydrates. Thermal analyses indicated that DDGS protein exhibits higher heat resistance than SPI, with thermal stability suggested by elevated onset and peak temperatures, and greater residual mass after decomposition in TGA, reflecting its higher mineral and lignocellulosic content. FTIR spectra further differentiated the two, with SPI showing prominent Amide I and II bands indicating pure, well-structured proteins, while DDGS protein spectra displayed broader bands associated with carbohydrates and lipids. Amino acid profiling confirmed SPI's superior amino acid profile, rich in essential amino acids like leucine, lysine, and phenylalanine, highlighting its high-quality protein status, whereas DDGS protein, though containing a similar profile, had lower amino acid concentrations overall. Collectively, these findings underscore the importance of optimized extraction conditions and reveal distinct structural, thermal, and nutritional characteristics of DDGS and SPI, with DDGS proteins being more suitable for enzymatic hydrolysis as they are in denatured state by ethanol processing which alter their molecular weight and structure increasing enzyme accessibility by exposing new reactive sites, whereas SPI being more appropriate for food formulations due to its purity and amino acid completeness.

Availability of Data and Materials

The datasets used and analyzed during the current study are available from the corresponding author on reasonable request.

Author Contributions

Conceptualization, Supervision, Resources, AH; Methodology, AH and MH; Software, MH; Validation, MH and AH; Writing original draft, MH; Funding acquisition, AH. Both authors have read and agreed to the final version of the manuscript. Both authors contributed to editorial changes in the manuscript. Both authors have participated sufficiently in the work and agreed to be accountable for all aspects of the work.

Ethics Approval and Consent to Participate

Not Applicable.

Acknowledgment

The authors would like to acknowledge the North Dakota State University Department of Agricultural and Biosystems Engineering for allowing the use of its laboratory facilities and equipment.

Funding

This research was funded by North Dakota Corn Counsil with grant number FAR0038727 and Higher Education Commission of Pakistan.

Conflicts of Interest

The authors declare no conflicts of interest.

References

[1] Abd El-Hac ME, Alagawany M, Fara MR, Dhama K. Use of maize distiller's dried grains with solubles (DDGS) in laying hen diets: trends and advances. Asian Journal of Animal and Veterinary Advances. 2015; 10: 690–707. https://doi.org/10.3923/ajava.2015.690.707.

[2] Iram A, Cekmecelioglu D, Demirci A. Distillers' dried grains with solubles (DDGS) and its potential as fermentation feedstock. Applied Microbiology and Biotechnology. 2020; 104: 6115–6128. https://doi.org/10.1007/s00253-020-10682-0.

[3] Rausch KD, Belyea RL, Ellersieck MR, Singh V, Johnston DB, Tumbleson ME. Particle size distributions of ground corn and DDGS from dry grind processing. Transactions of the ASAE. 2005; 48: 273–277. https://doi.org/10.13031/2013.17928.

[4] Buenavista RME, Siliveru K, Zheng Y. Utilization of distiller's dried grains with solubles: a review. Journal of Agriculture and Food Research. 2021; 5: 100195–100195. https://doi.org/10.1016/j.jafr.2021.100195.

[5] Kim Y, Mosier NS, Hendrickson R, Ezeji T, Blaschek H, Dien B, *et al*. Composition of corn dry-grind ethanol by-products: DDGS, wet cake, and thin stillage. Bioresource Technology. 2008; 99: 5165–5176. https://doi.org/10.1016/j.biortech.2007.09.028.

[6] Cookman DJ. Protein extraction from distiller's grain [Master's thesis]. Iowa State University: Ames, Iowa. 2008.

[7] Dong Y, Li Q, Gao N, Chen X, Cheng Y, Lu J, *et al*. Optimization of protein extraction from DDGS using response surface methodology and the properties of the protein. In 2012 Fifth International Conference on Intelligent Computation Technology and Automation (pp. 242–245). Zhangjiajie, Hunan, China. IEEE. 2012.

[8] Bezerra MA, Santelli RE, Oliveira EP, Villar LS, Escaleira LA. Response surface methodology (RSM) as a tool for optimization in analytical chemistry. Talanta. 2008; 76: 965–977. https://doi.org/10.1016/j.talanta.2008.05.019.

[9] Bello I, Adeniyi A, Mukaila T, Hammed A. Optimization of soybean protein extraction with ammonium hydroxide (NH4OH) using response surface methodology. Foods. 2023; 12: 1515–1515. https://doi.org/10.3390/foods12071515.

[10] Kruger NJ. The Bradford method for protein quantitation. In Walker JM (ed.) The protein protocols handbook (pp. 17–24). Humana Press: Totowa. 2009.

[11] Latimer GW. Official methods of analysis of AOAC International. 19th edn. AOAC International: Gaithersburg. 2012.

[12] Ismail BP. Ash content determination. In Nielsen SS, Ismail BP

(eds.) Nielsen's food analysis laboratory manual (pp. 129–131). Springer International Publishing: Cham. 2024.
[13] He Z, Zhang H, Olk DC, Shankle M, Way TR, Tewolde H. Protein and fiber profiles of cottonseed from upland cotton with different fertilizations. Modern Applied Science. 2014; 8: 97–103. https://doi.org/10.5539/mas.v8n4p97.
[14] Das D, Panesar PS, Saini CS. pH shifting treatment of ultrasonically extracted soybean meal protein isolate: effect on functional, structural, morphological and thermal properties. Process Biochemistry. 2022; 120: 227–238. https://doi.org/10.1016/j.procbio.2022.06.015.
[15] Official methods of analysis of AOAC International. 21st edn. AOAC International: Gaithersburg, MD, USA. 2019.
[16] Smith EP, Rose KA. Model goodness-of-fit analysis using regression and related techniques. Ecological Modelling. 1995; 77: 49–64. https://doi.org/10.1016/0304-3800(93)E0074-D.
[17] Ekpenyong M, Antai S, Asitok A, Ekpo B. Response surface modeling and optimization of major medium variables for glycolipopeptide production. Biocatalysis and Agricultural Biotechnology. 2017; 10: 113–121. https://doi.org/10.1016/j.bcab.2017.02.015.
[18] Ovando E, Rodríguez-Sifuentes L, Martínez LM, Chuck-Hernández C. Optimization of soybean protein extraction using by-products from NaCl electrolysis as an application of the industrial symbiosis concept. Applied Sciences. 2022; 12: 3113–3113. https://doi.org/10.3390/app12063113.
[19] Coelho TLS, Braga FMS, Silva NMC, Dantas C, Lopes Júnior CA, de Sousa SAA, *et al.* Optimization of the protein extraction method of goat meat using factorial design and response surface methodology. Food Chemistry. 2019; 281: 63–70. https://doi.org/10.1016/j.foodchem.2018.12.055.
[20] Phongthai S, Lim ST, Rawdkuen S. Ultrasonic-assisted extraction of rice bran protein using response surface methodology. Journal of Food Biochemistry. 2017; 41: e12314–e12314. https://doi.org/10.1111/jfbc.12314.
[21] Rosentrater KA, Zhang Y, Wrenn B. Impacts of ethanol production and drying conditions on the chemical, physical, and flowability properties of distillers dried grains with solubles. Frontiers in Bioengineering and Biotechnology. 2021; 9: 716634–716634. https://doi.org/10.3389/fbioe.2021.716634.
[22] Sui X, Zhang T, Jiang L. Soy protein: molecular structure revisited and recent advances in processing technologies. Annual Review of Food Science and Technology. 2021; 12: 119–147. https://doi.org/10.1146/annurev-food-062220-104405.
[23] Pahm AA, Pedersen C, Stein HH. Standardized ileal digestibility of reactive lysine in distillers dried grains with solubles fed to growing pigs. Journal of Agricultural and Food Chemistry. 2009; 57: 535–539. https://doi.org/10.1021/jf802047d.
[24] Ayadi FY, Rosentrater KA, Muthukumarappan K, Brown ML. Twin-screw extrusion processing of distillers dried grains with solubles (DDGS)-based yellow perch (Perca flavescens) feeds. Food and Bioprocess Technology. 2012; 5: 1963–1978. https://doi.org/10.1007/s11947-011-0535-5.
[25] Ellepola SW, Choi SM, Ma CY. Conformational study of globulin from rice (Oryza sativa) seeds by Fourier-transform infrared spectroscopy. International Journal of Biological Macromolecules. 2005; 37: 12–20. https://doi.org/10.1016/j.ijbiomac.2005.07.008.
[26] Gorinstein S, Zemser M, Friedman M, Rodrigues WA, Martins PS, Vello NA, *et al.* Physicochemical characterization of the structural stability of some plant globulins. Food Chemistry. 1996; 56: 131–138. https://doi.org/10.1016/0308-8146(95)00144-1.
[27] Yaqoob S, Cai D, Liu M, Zheng M, Zhao CB, Liu JS. Characterization of microstructure, physicochemical and functional properties of corn varieties using different analytical techniques. International Journal of Food Properties. 2019; 22: 572–582. https://doi.org/10.1080/10942912.2019.1596124.
[28] Escolano-Casado G, Fernández-Penas R, Fernandez-Sanchez JF, Gomez-Morales J, Mino L. Spectroscopic insights into the structural, surface and luminescence properties of Ca/Tb substituted phosphates. Available at SSRN. https://ssrn.com/abstract=5690793. (In preprint)
[29] Alesaeidi S, Kahrizi MS, Ghorbani Tajani A, Hajipour H, Ghorbani M. Soy Protein Isolate/Sodium Alginate Hybrid Hydrogel Embedded with Hydroxyapatite for Tissue Engineering. Journal of Polymers and the Environment. 2023; 31: 396-405. https://doi.org/10.1007/s10924-022-02635-7.
[30] Mingqiao C, Qinghua Y, Zhidan L. Development and Characterization of Soy Protein Isolate/Xylose Film. International Journal of Polymer Science. 2024; 1673547. https://doi.org/10.1155/2024/1673547.
[31] Tang CH, Chen Z, Li L, Yang XQ. Effects of transglutaminase treatment on the thermal properties of soy protein isolates. Food Research International. 2006; 39: 704–711. https://doi.org/10.1016/j.foodres.2006.01.012.
[32] Chen N, Zhao M, Chassenieux C, Nicolai T. Data on the characterization of native soy globulin by SDS-PAGE, light scattering and titration. Data in Brief. 2016; 9: 749–752. https://doi.org/10.1016/j.dib.2016.10.016.
[33] Xu W, Reddy N, Yang Y. An acidic method of zein extraction from DDGS. Journal of Agricultural and Food Chemistry. 2007; 55: 6279–6284. https://doi.org/10.1021/jf0633239.
[34] Jakobsen GV, Jensen BB, Knudsen KEB, Canibe N. Improving the nutritional value of rapeseed cake and wheat dried distillers grains with solubles by addition of enzymes during liquid fermentation. Animal Feed Science and Technology. 2015; 208: 198–213. https://doi.org/10.1016/j.anifeedsci.2015.07.015.